Supporting Online Material for

Spectrally-selective all-inorganic scattering luminophores for solar energy-harvesting clear glass windows

Ramzy Alghamedi, Mikhail Vasiliev, Mohammad Nur-E-Alam and Kamal Alameh

Electron Science Research Institute, Edith Cowan University, 270 Joondalup Drive, Joondalup, WA, 6027, Australia

*Corresponding author. E-mail: r.alghamedi@ecu.edu.au

Ensuring energy efficiency is a crucial requirement of modern architectural design practices. The demand for new construction materials with improved energy efficiency (including glass and glazings) is growing rapidly. The majority of established industrial PhotoVoltaic (PV) and other "green" technologies typically require allocation of large land areas outside cities, and are therefore not readily suitable for integration into built environments. An attractive way of improving the energy efficiency in buildings dramatically is represented by the emerging BIPV technologies. The ultimate form of integrating the energy generating PV installations into modern buildings proposed since the 1970's which has not yet been industrialized, is related to the implementation of Luminescent Solar concentration (LSC) technology concepts inside window glazing-based platforms. Luminescence and geometric light-trapping effects and spectrally-selective components for direct light deflection and scattering can be combined to pioneer practical transparent BIPV "solar windows". Our approach of re-directing the flow of unwanted non-visible solar radiation towards the frame-mounted cells offers the benefits of geometric flux concentration, reduction in the use of conventional electrical power, and allows engineering the required long glazing lifetimes exceeding 25 years (because it is possible to protect the PV cells, optical coatings and also the luminophores from exposure to environmental factors such as moisture, temperature, and cleaning chemicals).

The properties of inorganic luminophore mixes can be engineered to (i) efficiently convert the UV and part of the IR solar radiations into an IR band well-matched to the high-efficiency spectrum range of PV cells, (ii) scatter light with minimum optical attenuation, (iii) enhance light trapping within glazing structures and lamination interlayers and (iv) help guide the emitted and multiply scattered light along the lamination interlayer, using effects of total internal reflection and coating-assisted light guidance for collection by PV cells attached to the glass panel edges. The internal flux deflection mechanisms employed are related to multiple scattering, diffraction events and light diffusion. This results in preferential concentration of non-visible solar flux energy at glass panel edges, if a suitable IR-emitting luminophore combination is used in conjunction with spectrally-selective coating that can provide high reflectivity for the unpolarised IR light across a broad range of wavelengths and incidence angles. The effects of enhanced diffused transmission component across a wide spectral range, including the visible, originating from the presence of a quasi-random disordered structure inside interlayers can also be harnessed to improve energy output.

Our energy-harvesting clear glass panels employ a combination of inorganic photoluminescent materials, disorder-related light deflection mechanisms, and novel IR-specific optical interference coatings for solar radiation control (Fig. 1 within the main manuscript). We report on recently-developed high-transparency 100mm×100mm samples using inorganic luminophore powder mixes incorporated into lamination interlayers. We also focus on describing our sample testing methodologies and the results of luminescent interlayer's composition optimization for maximum electrical energy generation.

1. Luminophores selection and interlayer properties

We optimize the types and compositions of all-inorganic luminophore powders and demonstrate their capability to realize a visibly-transparent energy-harvesting clear laminated glass panel.

The types and chemistries of the four IR-emitting luminophore material compositions trialed are summarized in Table 1 within the main manuscript. We selected the luminescent materials each possessing a combination of all or some the

following properties of importance for our application: a) the presence of solar-IR excitation and/or near-IR emission wavelength bands; b) inorganic nature and high environmental and photo-exposure stability; c) large Stokes shift values, and d) availability of the required materials in the form of powders containing particles of size near 1 μm.

The main photoluminescence excitation and emission properties of luminophore α are described in Fig. S1. Note that this rare-earth-doped Y_2O_3-based luminophore powder also possessed narrow upconversion photoluminescence in the visible range when excited near 980 nm, however, its dominant near-IR emissions between 1000-1060 nm were reasonably well-matched to the high-efficiency spectrum range of PV conversion in $CuInSe_2$ (CIS) cells.

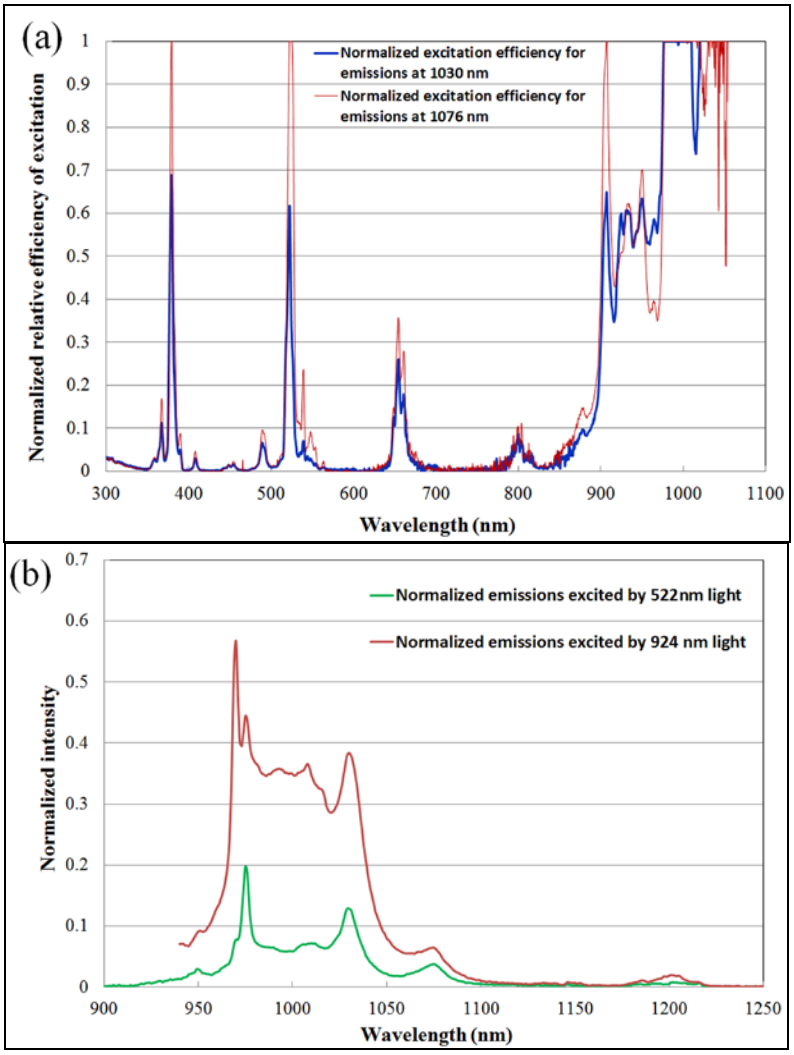

Figure S1. Measured near-infrared fluorescence excitation (a) and emission (b) spectra of yttria-based phosphor of composition α (data and measurements are courtesy of Edinburgh Instruments Ltd, Scotland, UK).

In the experiments, the active luminescent material layer (of optimized composition and thickness) was placed in-between two glass substrates. For electric power generation, a UV-curable, optically clear epoxy was used to glue CIS solar cells on all side edges of the functionalized laminated glass panes. Upon curing, the solar cells were electrically connected in parallel to generate an electric power output using conventional wiring in conjunction with a specialized soldering procedure adapted to making reliable connections with top conductive oxide layer of CIS modules.

2. Testing of luminophore suitability for redirecting emissions towards sample edge areas

In order to test and confirm the suitability of luminophore powders to function as luminescent energy converters within the glass structures connected by thin luminophore-loaded epoxy interlayers, direct optical measurements of excitation-emission matrices of epoxy-luminophore layers were carried out. The composite-type luminescent medium of dimensions 50x50x1 mm^3 was placed in-between uncoated glass plates. Figure S2 provides the details on the experimental procedures used as well as measured spectral parameters of luminescence for the interlayers containing a small (< 1wt%) concentration of a custom-made high-performance specialized luminophore γ (its composition is described as ZnS : (Ag, Tm)).

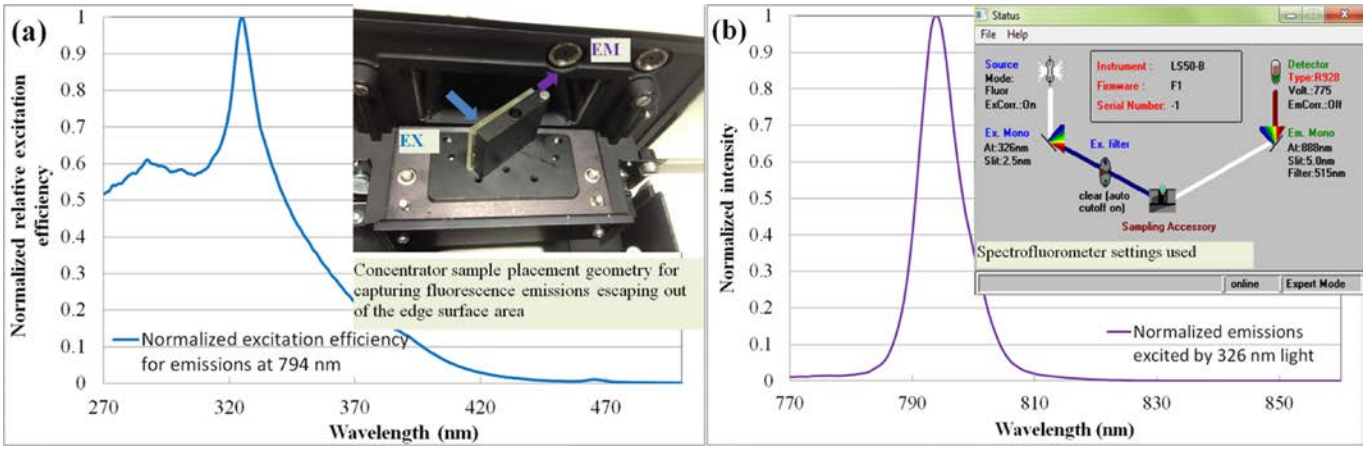

Figure S2. Measurements of the excitation and emission spectra of epoxy-based lamination interlayers containing suspended particles of ZnS : (Ag, Tm) (luminophore γ). A Perkin-Elmer LS-50B luminescence spectrometer was used to collect and analyze the optical radiation flux propagating out of an edge area of 50x50x3mm^3 concentrator samples composed of two 1mm-thick Corning glass plates connected via a UV-cured functionalized epoxy interlayer. Luminophore particles were dispersed uniformly within liquid epoxy at concentrations not exceeding 1 wt%. Strong emission intensities were observed near 794 nm, almost saturating the spectrometer detection system, under normal-incidence UV excitation and when the sample edge area aperture was aligned with the input aperture of the emissions monochromator.

3. Sample preparation and component properties

The mean particle size varied between 0.5-2.5 μm for the different powders, after dry grinding for several hours using Fritsch Pulverisette Premium Line 7 ball mill, and their solubilities in UV-curable optical epoxies varied depending on the material type and particle size. However, it was possible to form 1mm or even 2mm thick cured almost-clear interlayers containing up to 0.1-0.3 wt% of total powder concentration loading; both Norland NOA61 and WTS-80203 single-component clear epoxies were found to function as suitable host matrices for the luminescent materials, and the same epoxies were also used to attach the solar cell surfaces to the glass edges.

After the functionalized lamination layers were cured, CIS solar cell module cut-outs of size 100mm×25 mm were glued to the edges and parallel-connected electric circuits were formed in which each cell in a bundle of four side-mounted cells was used in conjunction with a blocking diode that prevents backfeed DC currents. To alleviate the shadowing-related issues, which are to an extent intrinsic for edge-mounted PV modules used in solar concentrator devices of the described type, we always connected the modules attached to each of the four sample sides in parallel. In all 100mm×100 mm concentrator samples (and also in 200mm×200mm samples which will be reported elsewhere), each sample side had only one CIS module attached to it. The cut-outs were produced using standard glass cutting techniques and the original CIS module size was 200mm×270 mm. The $CuInSe_2$ thin-film solar cells on 2 mm glass substrates had nominal rated efficiency of 9.2% (at 25ºC) and their Fill Factor (*FF*) was about 60%. The module cut-outs were supplied as integrated internally series-connected CIS cell sequences, so that each module cut-out of length 100 mm had a saturated open-circuit voltage (V_{oc}) near 7.8 V. Their Nominal Operating Cell Temperature (*NOCT*) is 47 °C and the temperature coefficient of output power 0.31 %/°C. CIS modules were used instead of silicon cells because of their extended range (up to 1220 nm) of spectral sensitivity and the relative stability of output with respect to active-area shading of cells. It is important to note that the cell-shadowing-related performance aspects relevant to the electrical circuit engineering features are also crucial for the design of practical LSC-type concentrators for glass industry applications.

4. Experimental data and results

Calculations performed according to Equation (2) in the main manuscript using the integration limits between 300 nm and 1220 nm show that the total optical power ($P_{refl,opt}$) within the bandwidth of interest (for 2″ diameter incident beam) after its first reflection off the coating was only 532.6 mW, or 26% of the total optical power within the incident beam. This figure emphasizes the trade-off between the amount of optical power that can be routed towards edges and the transparency of the energy harvesting clear glass and justifies the relatively moderate flux concentration performance obtained in LSC-type devices of substantial visible-range transparency.

The measured electric output data used to calculate *ACG* (defined by equation (1) in the main manuscript) and other light concentration efficiency-related parameters are shown in Table S1.

Table S1. Electric output parameters measured for all samples under the simulated AM1.5G illumination conditions using a normally-incident collimated 2″ diameter beam and the same beam diffused by a dot-patterned glass plate.

Incidence geometry	Collimated beam		Diffused beam		(Icc*Voc*FF)/$A_{tot,\ cells}$ (Collimated beam case)
Sample ID	I_{sc} (mA)	V_{oc} (V)	I_{sc} (mA)	V_{oc} (V)	
A	0.8	2.02	0.6	1.92	0.0097
B	1.1	1.53	0.93	1.53	0.0101
C	1.64	4.04	1.43	3.98	0.0398
D	2.98	4.59	2.43	4.27	0.0821
E	3.21	5.12	2.52	4.93	0.0986
F	2.03	4.45	1.75	4.05	0.0542
G	2.1	4.56	1.75	4.34	0.0575
H	3.31	3.98	2.67	4.06	0.0790
I	1.71	4.39	1.4	4.13	0.0450
J	2.58	5.14	2.26	4.8	0.0796
K	2.0	5.51	1.61	4.93	0.0661
L	1.15	4.69	0.94	4.37	0.0324

The *ACG* and also *DEF* values for all samples have been calculated using the methodologies described within the manuscript and the data of Table S1.

Thermal insulation and solar control properties

The thermal insulation, solar heat shielding and solar radiation control performance of our glazing systems (employing the low-emissivity high spectral selectivity solar-control coatings described in Fig. 1(c) of the main manuscript) were characterized computationally using Lawrence Berkeley National Laboratory's (LBNL) Optics 6.0 and WINDOW 6.3 software packages. The solar heat gain coefficient (SHGC) of our transparent glazings is around 0.41, placing them among the industry-leading coated glazing systems in terms of solar control performance, especially considering that the Light-to-Solar Gain (LSG) parameter exceeds 1.8. The thermal insulation U-factor value was < 1.8 W/(m^2K) for insulating glass units containing a 0.5″ air space in conjunction with the basic glazing structure of Fig 1(a) in the main manuscript. Note that the relatively high SHGC value of 0.41 is due exclusively to the high transparency properties of the glass coated with our metal-dielectric films.